Punjab University Journal of Mathematics (2025), 57(07), 706-726
https://doi.org/10.52280/pujm.2025.57(07)01

Design and Analysis of a Combined 4-Point Ternary Refinement Scheme with C^4-Smoothness

Received
05 May, 2025

Accepted
10 November, 2025

Published Online
17 December, 2025

*Pakeeza Ashraf
Department of Mathematics,
Government Sadiq College Women University, Bahawalpur, Pakistan

Fatima Rasheed
Department of Mathematics,
Government Sadiq College Women University, Bahawalpur, Pakistan

Abstract. In this paper, we introduce a new combined four-point ternary refinement scheme capable of generating both interpolating and approx-imating curves. The scheme is constructed by translating a quintic B-Spline refinement scheme to new positions using displacement vectors that incorporate four shape control parameters. We demonstrate that this combined scheme produces limit curves with up to C^4 continuity and al-so provides significant flexibility in crafting smooth curves with reduced support size. Furthermore, we establish that various well-known inter-polatory and approximating refinement schemes are special cases of our proposed approach. Some key properties, including polynomial generation, reproduction, and support width, are examined. Additionally, we investigate the fractal generation characteristics of the refinement scheme, revealing that specific parameter choices enable effective construction of fractal curves. Through a series of numerical experiments, we validate that the limit curves produced by our scheme accurately reflect the associ-ated control polygons, yielding more realistic results compared to existing methods.

AMS (MOS) Subject Classification Codes: 65D17; 65D10; 65D07; 65D05
Key Words: Refinement scheme; combined ; continuity; shape-control; fractals.

1. Introduction

Computer Aided Geometric Design (CAGD) deals with the mathematical representation, animation and construction of curves and surfaces. Refinement is an essential tool for curve and surface modeling in CAGD. A refinement scheme constructs a curve from a polygon or a surface from a mesh by iteratively subdividing them according to specific subdivision rules. This recursive process yields a limiting curve or surface that achieves the smoothness required for various applications. In each iteration, the position of new vertices is estimated using the subdivision matrix, where each new vertex is calculated as a weight-ed sum of the vertices from the previous level.

**Corresponding Author*: pakeeza@gscwu.edu.pk

Refinement schemes can be divided into two types based on their application: interpolating and approximating schemes. Both types have distinct advantages. Interpolating schemes are constrained to pass through all initial control points, making them particularly useful in specific industrial applications. Founda-tional studies on interpolating refinement schemes can be found in [6, 5, 1]. On the other hand, approximating schemes facilitate intersection operations and generate curves with higher smoothness and continuity. Significant contributions on approximating schemes are detailed in [10, 7, 12]. Recent developments on stationary and non-stationary refinement schemes are highlighted in [2, 11, 25].

The concept of combining schemes was pioneered by Levin [13], who introduced a combined refinement scheme for interpolating nets of curves in parametric form. Since then, several advancements have followed. Pan et al. [18] developed a C^2-continuous combined refinement scheme. Novara and Romani [17] proposed a ternary combined scheme that ensures C^3 continuity, whereas Rehan and Sabri [20] extended this idea to a ternary 4-point scheme with a shape parameter, allowing local control over curve behavior. Zhang et al. [24] further enriched this direction by incorporating multiple shape parameters in a ternary combined 4-point scheme.

In parallel, the connection between subdivision schemes and fractal geometry has drawn considerable attention. Fractal curves, characterized by self-similarity across scales, are instrumental in modeling naturally irregular objects such as coastlines, mountain terrains, and biological structures like blood vessels and bronchial trees. Subdivision schemes have been found to efficiently generate such fractal curves from discrete control points. Zheng et al. [26] explored the fractal behavior of binary 4-point and ternary 3-point interpolatory schemes.

Peng et al. [19] extended this line of research by analyzing the fractal characteris-tics of ternary interpolatory and rational schemes, including the impact of shape parameters on fractal dimensions. Rehan and Siddiqi [21] analyzed the combined binary 6-point subdivision scheme with tension parameters. Yao et al. [23] examined the geometric properties of a quaternary 4-point interpolatory scheme.

1.1. **Motivation and Contribution.** The above literature reveals two important trends:

- Most combined refinement schemes incorporate at most one or two shape parameters, limiting their flexibility in achieving diverse curve shapes and geometric properties.
- Research on the fractal characteristics of refinement schemes is predominantly focused on interpolatory schemes, with limited exploration of combined schemes in this context.

These gaps motivate the present work. We propose a novel family of combined refinement schemes characterized by multiple shape parameters, enabling the generation of both interpolating and approximating limit curves. The proposed scheme not only subsumes various existing schemes as special cases but also provides an efficient mechanism for generating fractal curves by appropriately choosing parameter values. This framework introduces enhanced flexibility and control, making it a powerful tool for applications in geometric

design, computer graphics, and fractal modeling.
The remainder of this paper is organized as follows: Section 2 introduces the necessary preliminary definitions and notations used throughout the paper. In Section 3, we present the construction of the proposed refinement scheme along with its parametric formulation. Section 4 explores the theoretical properties of the scheme, including support, smoothness, and polynomial generation and reproduction. In Section 5, we investigate the fractal behavior of the scheme under specific parametric choices. Section 6 provides numerical experiments to validate the performance and flexibility of the proposed scheme and section 7 concludes the paper with a summary of the main contributions.

2. Notations and Preliminaries

Initially, given a sequence of control points $b^0 = \{b_i^0 \in \mathbb{R}\}$. Let $b^k = \{b_i^k \in \mathbb{R}\}_{i\in\mathbb{Z}}$ be the set of control points at level $k(k \geq 0, k \in \mathbb{Z})$ and satisfy these rules recursively:

$$b_i^{k+1} = \sum_{j\in\mathbb{Z}} l_{i-3j} b_j^k, i \in \mathbb{Z}. \tag{2. 1}$$

$L = \{l_i\}_{i\in\mathbb{Z}}$ be the subdivision mask and $L(z) = \sum_{i\in\mathbb{Z}} l_i z^i$, is known as the Laurent polynomial.
A refinement scheme S is convergent if for every initial point $b^0 = \{b_i^0 \in \mathbb{R}\}$, there exist a continuous function $p \in C(\mathbb{R})$ such that for every compact set $I \subseteq \mathbb{R}$, it satisfies

$$\lim_{x\to\infty} \max_{i\in\mathbb{Z}\cap 3^k l} |b_i^k - p(3^{-k}i)| = 0,$$

and $p \neq 0$ for some initial data b^0. The function p defined as, $p = S^\infty b^0$ is considered to be a limit function of the refinement scheme S. For the convergent refinement scheme S, the corresponding mask definitely satisfies

$$\sum_{i\in\mathbb{Z}} l_{3i} = \sum_{i\in\mathbb{Z}} l_{3i+1} = \sum_{i\in\mathbb{Z}} l_{3i+2} = 1. \tag{2. 2}$$

Suppose a refinement scheme S with $L = \{l_i\}_{i\in\mathbb{Z}}$ satisfies (2. 2), then there exists S_1 (first order difference scheme of S) which satisfies

$$db^k = S_1 db^{k-1},$$

where

$$b^k = S^k b^0, \quad db^k = \{(db^k)_i = 3^k(b_{i+1}^k - b_i^k) | i \in \mathbb{Z}\}.$$

The symbol of S_1 is

$$L^{(1)}(z) = \frac{3z^2}{1+z+z^2} L(z).$$

Further, if S_m is the m^{th} order difference scheme of S with $L^{(m)} = \{l^{(m)}\}_{i\in\mathbb{Z}}$, then the symbol of S_m is

$$L^{(m)}(z) = \left(\frac{3z^2}{1+z+z^2}\right) L(z).$$

If there exist an integer $M \geq 1$, such that

$$\left\| \left(\frac{1}{3} S_{m+1} \right)^M \right\|_\infty < 1,$$

then the scheme S is C^m- continuous, where

$$\left\| \left(\frac{1}{3} S_{m+1} \right)^M \right\|_\infty = \left\{ \max \sum_{j \in \mathbb{Z}} \left| \left(\frac{1}{3} l^{(m+1)}_{3^M j+i} \right)^{(M)} \right| : i = 0, 1, \cdots, 3^M - 1 \right\}.$$

3. CONSTRUCTION OF THE T_4- SCHEME

In this section, we present our combined four-point ternary refinement scheme. The proposed scheme is constructed by directly adding the displacement vectors into the geometric rules of quintic B-spline ternary refinement scheme with C^2- convergence. The matrix form of the refinement scheme is expressed as

$$\begin{pmatrix} \acute{b}^{k+1}_{3i} \\ \acute{b}^{k+1}_{3i+1} \\ \acute{b}^{k+1}_{3i+2} \end{pmatrix} = \begin{pmatrix} \frac{1}{243} & \frac{50}{243} & \frac{47}{81} & \frac{50}{243} & \frac{1}{243} \\ 0 & \frac{7}{81} & \frac{14}{27} & \frac{10}{27} & \frac{2}{81} \\ 0 & \frac{2}{81} & \frac{10}{27} & \frac{14}{27} & \frac{7}{81} \end{pmatrix} \begin{pmatrix} b^k_{i-1} \\ b^k_i \\ b^k_{i+1} \\ b^k_{i+2} \end{pmatrix}. \tag{3. 3}$$

Let Δb^k_{i-1}, Δb^k_i, Δb^k_{i+1}, be the displacement vectors and represents the change in position in control points. Let α, β, ν and λ $(\alpha, \beta, \nu, \lambda \in \mathbb{R})$ be the shape parameters which control the size and direction of the displacement vectors. By adding these shape parameters and displacement vectors into (3. 3), we get

$$\begin{pmatrix} b^{k+1}_{3i} \\ b^{k+1}_{3i+1} \\ b^{k+1}_{3i+2} \end{pmatrix} = \begin{pmatrix} \acute{b}^{k+1}_{3i} \\ \acute{b}^{k+1}_{3i+1} \\ \acute{b}^{k+1}_{3i+2} \end{pmatrix} + \begin{pmatrix} \alpha & \beta & \alpha \\ 0 & \nu & \lambda \\ 0 & \lambda & \nu \end{pmatrix} \begin{pmatrix} \Delta b^k_{i-1} \\ \Delta b^k_i \\ \Delta b^k_{i+1} \end{pmatrix},$$

where

$$\begin{pmatrix} \Delta b^k_{i-1} \\ \Delta b^k_i \\ \Delta b^k_{i+1} \end{pmatrix} = \begin{pmatrix} -b^k_{i-2} + 2b^k_{i-1} - b^k_{i-1} \\ -b^k_{i-1} + 2b^k_i - b^k_{i+1} \\ -b^k_i + 2b^k_{i+1} - b^k_{i+2} \end{pmatrix}.$$

Thus, the combined 4-point ternary refinement scheme (*T_4-scheme*) can be generated as

$$\begin{cases} b^{k+1}_{3i} = \left(\frac{1}{243} - \alpha\right) b^k_{i-2} + \left(\frac{50}{243} + 2\alpha - \beta\right) b^k_{i-1} + \left(\frac{47}{81} - 2\alpha + 2\beta\right) b^k_i \\ \qquad\quad + \left(\frac{50}{243} + 2\alpha - \beta\right) b^k_{i+1} + \left(\frac{1}{243} - \alpha\right) b^k_{i+2}, \\ b^{k+1}_{3i+1} = \left(\frac{7}{81} - \nu\right) b^k_{i-1} + \left(\frac{14}{27} + 2\nu - \lambda\right) b^k_i + \left(\frac{10}{27} - \nu + 2\lambda\right) b^k_{i+1} + \left(\frac{2}{81} - \lambda\right) b^k_{i+2}, \\ b^{k+1}_{3i+2} = \left(\frac{2}{81} - \lambda\right) b^k_{i-1} + \left(\frac{10}{27} - \nu + 2\lambda\right) b^k_i + \left(\frac{14}{27} + 2\nu - \lambda\right) b^k_{i+1} + \left(\frac{7}{81} - \nu\right) b^k_{i+2}. \end{cases} \tag{3. 4}$$

Consequently, the Laurent polynomial of the T_4-*scheme* is expressed as

$$\begin{aligned} L(z) &= \left(\frac{1}{243}-\alpha\right)(z^6+z^{-6})+\left(\frac{2}{81}-\lambda\right)(z^5+z^{-5})+\left(\frac{7}{81}-\nu\right)(z^4+z^{-4})+\left(\frac{50}{243}+\right. \\ &\quad \left.2\alpha-\beta\right)(z^3+z^{-3})+\left(\frac{10}{27}-\nu+2\lambda\right)(z^2+z^{-2})+\left(\frac{14}{27}+2\nu-\lambda\right)(z+z^{-1})+ \\ &\quad \left(\frac{47}{81}-2\alpha+2\beta\right). \end{aligned} \tag{3. 5}$$

3.1. **Special cases of the T_4-scheme.** The T_4-*scheme* involves four independent parameters. The provided scheme has many existing ternary schemes with defined parameters. Here we enlist some special cases of the T_4-scheme.

- The scheme given in [9] become the special case of the T_4-scheme, for $(\alpha,\beta,\nu,\lambda) = (\frac{1}{243}, \frac{52}{243}-\frac{1}{9}\alpha, \frac{7}{81}, \frac{2}{81})$.
- The scheme given in [16] become the special case of the T_4-scheme, for $(\alpha,\beta,\nu,\lambda) = (\frac{1}{243}, \frac{1}{9}(\frac{25}{27}-\frac{1}{4}\alpha), \frac{1}{9}(\frac{7}{9}-\frac{1}{4}\alpha), \frac{2}{81})$.
- The scheme given in [22] become the special case of the T_4-scheme, for $(\alpha,\beta,\nu,\lambda) = (\frac{1}{243}+\mu, \frac{52}{243}-2\mu, \frac{4}{27}, \frac{2}{27})$.
- The scheme given in [18] become the special case of the T_4-scheme, for $(\alpha,\beta,\nu,\lambda) = (\frac{1}{243}, \frac{16}{243}-\frac{1}{27}\alpha, \frac{4}{27}-\beta(1-\alpha), \frac{2}{27}-\beta(1-\alpha))$.
- The scheme given in [17] become the special case of the T_4-scheme, for $(\alpha,\beta,\nu,\lambda) = (\frac{1}{243}, \frac{25}{243}+\alpha, \frac{7}{81}-\beta, \frac{2}{81}-\gamma)$.

Table 1 summarizes the special cases of the T_4-*scheme*.

4. PROPERTIES OF THE T_4- SCHEME

In this section, we investigate some significant properties of the T_4-*scheme*, including continuity, support, polynomial generation/reproduction, and approximating order.

4.1. **Continuity analysis.** We analyze continuity of the T_4-*scheme*. For refinement schemes, continuity analysis is essential question. The smoothness of the scheme depends on the continuity of the scheme.

Theorem 4.2. *The* T_4-scheme *defined by (3. 4) produces up to* C^4*- limit curve. Then,*
(i) it produces C^0*-limit curve when*

$$\begin{aligned} &\alpha,\beta,\lambda,\nu \in \{\alpha,\beta,\nu,\lambda\in\mathbb{R}, \max\{\left|\frac{1}{243}-\alpha\right|+\left|\frac{10}{81}+\alpha-\beta+\nu\right|+\left|\frac{5}{27}-\alpha+\beta-\nu+\lambda\right| \\ &+\left|\frac{5}{243}-\alpha-\lambda\right|, 2\left|\frac{5}{81}-\nu+\lambda\right|+\left|\frac{17}{81}+2\nu-2\lambda\right|\} < 1\}; \end{aligned}$$

(ii) it produces C^1*-limit curve when*

$$\begin{aligned} &\alpha,\beta,\nu,\lambda \in \{\alpha,\beta,\nu,\lambda\in\mathbb{R}, \nu=0, \max\{\left|\frac{1}{81}-3\alpha\right|+\left|\frac{16}{81}-3\beta-3\lambda\right|+\left|\frac{10}{81}-3\alpha+6\lambda\right|, \\ &2\left|\frac{4}{81}+6\alpha-3\lambda\right|+\left|\frac{19}{81}+6\beta\right|\} < 1\}; \end{aligned}$$

(iii) it produces C^2-limit curve when

$$\alpha,\beta,\nu,\lambda\in\{\alpha,\beta,\nu,\lambda\in\mathbb{R},\beta=\lambda+\nu-2\alpha,\max\{\left|\frac{1}{9}+27\alpha-9\lambda\right|+\left|\frac{2}{9}-27\alpha-9\nu+27\lambda\right|,$$
$$2\left|\frac{1}{27}-9\alpha\right|+\left|\frac{7}{27}+18\alpha+18\nu-36\lambda\right|\}<1\};$$

(iv) it produces C^3-limit curve when

$$\alpha,\beta,\nu,\lambda\in\{\alpha,\beta,\nu,\lambda\in\mathbb{R},\beta=3\lambda-2\alpha,\nu=2\lambda,\max\{\left|\frac{1}{9}-27\alpha\right|+\left|\frac{2}{9}+108\alpha-27\lambda\right|,$$
$$\left|\frac{1}{3}-162\alpha+54\lambda\right|\}<1\};$$

(v) it produces C^4-limit curve when

$$\alpha,\beta,\nu,\lambda\in\{\alpha,\beta,\nu,\lambda\in\mathbb{R},-\frac{2}{243}<\alpha<\frac{1}{243},\beta=7\alpha,\nu=6\alpha,\lambda=3\alpha\}.$$

Proof. The Laurent polynomial plays a fundamental role in evaluating the continuity of the limit curve. The Laurent polynomial of the scheme is expressed as

$$\begin{aligned}L(z) &= \left(\frac{1}{243}-\alpha\right)(z^6+z^{-6})+\left(\frac{2}{81}-\lambda\right)(z^5+z^{-5})+\left(\frac{7}{81}-\nu\right)(z^4+z^{-4})+\left(\frac{50}{243}+\right.\\ &\left.2\alpha-\beta\right)(z^3+z^{-3})+\left(\frac{10}{27}-\nu+2\lambda\right)(z^2+z^{-2})+\left(\frac{14}{27}+2\nu-\lambda\right)(z+z^{-1})+\\ &\left(\frac{47}{81}-2\alpha+2\beta\right).\end{aligned}$$

As we know that

$$L^{(m)}(z) = \left(\frac{3z^2}{1+z+z^2}\right)L^{(m-1)}(z)=\left(\frac{3z^2}{1+z+z^2}\right)^m L(z),\quad z\in\mathbb{C}\backslash 0. \quad (4.\ 6)$$

(i) If we put $m=1$ in (4. 6), then we get

$$\frac{1}{3}L^{(1)}(z)=\frac{1}{3}\left(\frac{3z^2}{1+z+z^2}\right)L(z)=\sum_{i=-4}^{6}\vartheta_i z^i,$$

where $\vartheta_{-4}=\vartheta_6=\frac{1}{243}-\alpha$, $\vartheta_{-3}=\vartheta_5=\frac{5}{243}+\alpha-\lambda$, $\vartheta_{-2}=\vartheta_4=\frac{5}{81}-\nu+\lambda$, $\vartheta_{-1}=\vartheta_3=\frac{10}{81}+\alpha-\beta+\nu$, $\vartheta_0=\vartheta_2=\frac{5}{27}-\alpha+\beta-\nu+\lambda$, $\vartheta_1=\frac{17}{81}+2\nu-2\lambda$.
when

$$\alpha,\beta,\lambda,\nu\in\{\alpha,\beta,\nu,\lambda\in\mathbb{R},\max\{\left|\frac{1}{243}-\alpha\right|+\left|\frac{10}{81}+\alpha-\beta+\nu\right|+\left|\frac{5}{27}-\alpha+\beta-\nu+\lambda\right|$$
$$+\left|\frac{5}{243}-\alpha-\lambda\right|,2\left|\frac{5}{81}-\nu+\lambda\right|+\left|\frac{17}{81}+2\nu-2\lambda\right|\}<1\};$$

we obtain

$$\left\|\frac{1}{3}S_1\right\|_\infty=\frac{1}{3}\max\left\{\sum|l^{(1)}_{3i+j}|:j=0,1,2\right\}<1.$$

As we observe from $\left\|\frac{1}{3}S_1\right\|_\infty < 1$, the scheme is C^0 continuous.
(ii) By substituting $m = 2$ in (4. 6) , if $\nu = 0$, we get

$$\frac{1}{3}L^{(2)}(z) = \frac{1}{3}\left(\frac{3z^2}{1+z+z^2}\right)^2 L(z) = \sum_{i=-2}^{6} \vartheta_i z^i. \tag{4. 7}$$

where $\vartheta_{-2} = \vartheta_6 = \frac{1}{81} - 3\alpha$, $\vartheta_{-1} = \vartheta_5 = \frac{4}{81} + 6\alpha - 3\lambda$, $\vartheta_0 = \vartheta_4 = \frac{10}{81} - 3\alpha + 6\lambda$, $\vartheta_1 = \vartheta_3 = \frac{16}{81} - 3\beta - 3\lambda$, $\vartheta_2 = \frac{19}{81} + 6\beta$.
when

$$\alpha, \beta, \nu, \lambda \in \{\alpha, \beta, \nu, \lambda \in \mathbb{R}, \nu = 0, \max\{\left|\frac{1}{81} - 3\alpha\right| + \left|\frac{16}{81} - 3\beta - 3\lambda\right| + \left|\frac{10}{81} - 3\alpha + 6\lambda\right|,$$
$$2\left|\frac{4}{81} + 6\alpha - 3\lambda\right| + \left|\frac{19}{81} + 6\beta\right|\} < 1\};$$

we obtain

$$\left\|\frac{1}{3}S_2\right\|_\infty = \frac{1}{3}\max\left\{\sum |l^{(2)}_{3i+j}| : j = 0, 1, 2\right\} < 1.$$

As we see $\left\|\frac{1}{3}S_2\right\|_\infty < 1$,then the scheme is C^1 continuous.
(iii) By setting $m = 3$ in (4. 6) , if $\beta = \lambda + \nu - 2\alpha$, we have

$$\frac{1}{3}L^{(3)}(z) = \frac{1}{3}\left(\frac{3z^2}{1+z+z^2}\right)^3 L(z) = \sum_{i=0}^{6} \vartheta_i z^i. \tag{4. 8}$$

where $\vartheta_0 = \vartheta_6 = \frac{1}{27} - 9\alpha$, $\vartheta_1 = \vartheta_5 = \frac{1}{9} + 27\alpha - 9\lambda$, $\vartheta_2 = \vartheta_4 = \frac{2}{9} - 27\alpha - 9\nu + 27\lambda$, $\vartheta_3 = \frac{7}{27} + 18\alpha + 18\nu - 36\lambda$.
when

$$\alpha, \beta, \nu, \lambda \in \{\alpha, \beta, \nu, \lambda \in \mathbb{R}, \beta = \lambda + \nu - 2\alpha, \max\{\left|\frac{1}{9} + 27\alpha - 9\lambda\right| + \left|\frac{2}{9} - 27\alpha - 9\nu + 27\lambda\right|,$$
$$2\left|\frac{1}{27} - 9\alpha\right| + \left|\frac{7}{27} + 18\alpha + 18\nu - 36\lambda\right|\} < 1\};$$

we obtain

$$\left\|\frac{1}{3}S_3\right\|_\infty = \frac{1}{3}\max\left\{\sum |l^{(3)}_{3i+j}| : j = 0, 1, 2\right\} < 1.$$

As we see $\left\|\frac{1}{3}S_3\right\|_\infty < 1$, then the scheme is C^2 continuous.
(iv) By putting $m = 4$ in (4. 6) , if $\beta = 3\lambda - 2\alpha, \nu = 2\lambda$, we have

$$\frac{1}{3}L^{(4)}(z) = \frac{1}{3}\left(\frac{3z^2}{1+z+z^2}\right)^4 L(z) = \sum_{i=2}^{6} \vartheta_i z^i. \tag{4. 9}$$

where $\vartheta_2 = \vartheta_6 = \frac{1}{9} - 27\alpha$, $\vartheta_3 = \vartheta_5 = \frac{2}{9} + 108\alpha - 27\lambda$, $\vartheta_4 = \frac{1}{3} - 162\alpha + 54\lambda$.
when

$$\alpha, \beta, \nu, \lambda \in \{\alpha, \beta, \nu, \lambda \in \mathbb{R}, \beta = 3\lambda - 2\alpha, \nu = 2\lambda, \max\{\left|\frac{1}{9} - 27\alpha\right| + \left|\frac{2}{9} + 108\alpha - 27\lambda\right|,$$
$$\left|\frac{1}{3} - 162\alpha + 54\lambda\right|\} < 1\};$$

we obtain

$$\left\|\frac{1}{3}S_4\right\|_\infty = \frac{1}{3}\max\left\{\sum|l^{(4)}_{3i+j}| : j = 0,1,2\right\} < 1.$$

As we observe that $\left\|\frac{1}{3}S_4\right\|_\infty < 1$, then the scheme is C^3 continuous.
(v) After substituting $m = 5$ in (4. 6) , if $\beta = 7\alpha, \lambda = 3\alpha, \nu = 6\alpha$,
we have

$$\frac{1}{3}L^{(5)}(z) = \frac{1}{3}\left(\frac{3z^2}{1+z+z^2}\right)^5 L(z) = \sum_{i=4}^{6}\vartheta_i z^i. \tag{4. 10}$$

where $\vartheta_4 = \vartheta_6 = \frac{1}{3} - 81\alpha, \vartheta_5 = \frac{1}{3} + 162\alpha$.
when

$$\alpha,\beta,\nu,\lambda \in \{\alpha,\beta,\nu,\lambda \in \mathbb{R}, -\frac{2}{243} < \alpha < \frac{1}{243}, \beta = 7\alpha, \nu = 6\alpha, \lambda = 3\alpha\}.$$

We obtain

$$\left\|\frac{1}{3}S_5\right\|_\infty = \frac{1}{3}\max\left\{\sum|l^{(5)}_{3i+j}| : j = 0,1,2\right\} < 1.$$

As we see $\left\|\frac{1}{3}S_5\right\|_\infty < 1$, then the scheme is C^4-continuous. When $L^{(6)}(z)$ is evaluated, we do not obtain the Laurent polynomial. Hence, this indicates that the T_4-*scheme* is C^4-continuous. □

Table 2 shows the relationship between the continuity orders of limit curves and variation of parameters.

Experiment 4.3. In this experiment, we analyze limiting curves with the same control polygon while varying the continuity orders. The values of parameters are chosen from the respective continuity ranges. Figure $1(a)$ illustrates C^1 limiting curve for $\alpha = -\frac{1}{27}$, $\beta = \frac{1}{23}$, $\lambda = -\frac{1}{81}$ and $\nu = 0$. Figure $1(b)$ illustrates C^2 limiting curve for $\alpha = -\frac{1}{69}$, $\beta = -\frac{5033}{104880}$, $\lambda = -\frac{3}{80}$ and $\nu = -\frac{3}{76}$. Figure 1 (c) illustrates C^3 limiting curve for $\alpha = -\frac{1}{69}$, $\beta = -\frac{503}{4071}$, $\lambda = -\frac{3}{59}$ and $\nu = -\frac{6}{59}$. Furthermore, Figure $1(d)$ illustrates C^4 limiting curve for $\alpha = -\frac{1}{99}$, $\beta = -\frac{32}{297}$, $\lambda = -\frac{38}{891}$ and $\nu = -\frac{76}{891}$.

4.4. **Support of the T_4-*scheme*.** Support of a refinement scheme measures the effect by moving a single vertex from its location on its neighboring points. The support size of a scheme indicates the influence of local control on the limiting curves. Practically, smaller support size is more ideal in the applications of refinement schemes. Let us evaluate the basis function for determining the support size. We represent β as the limit function which comes from the initial data

$$\delta_i^0 = \begin{cases} 1, & i = 0, \\ 0, & i \neq 0\ . \end{cases} \tag{4. 11}$$

β is usually called the basic limit function of the scheme.

Theorem 4.5. *The support size of the basic limit function of the* T_4-scheme *is* $[-3, 3]$.

Proof. To determine the support size of β, we calculate the gap between the leftmost and rightmost non-zero vertices. When $k = 0$, with the help of (3. 4) and (4. 11), we get b^1_{-6}, b^1_{-5}, ..., b^1_5, b^1_6, as sequence of non-zero vertices.
By observing this, we define a set $G_k = \left\{ \frac{i}{3^k} : \forall\, i \in \mathbb{Z} \right\}$, where $\beta\left(\frac{i}{3^k}\right) = b^k_i, \forall\, i \in \mathbb{Z}$. We also determine that after the first refinement step, the non-zero leftmost vertex is $\beta\left(-\frac{6}{3}\right) = b^1_{-6}$, and the rightmost vertex is $\beta\left(\frac{6}{3}\right) = b^1_6$.
Similarly, after the second refinement step, the non-zero leftmost vertex is $\beta\left(-\frac{6(1+3)}{3^2}\right) = b^2_{-6(1+3)}$, and the rightmost vertex is $\beta\left(\frac{6(1+3)}{3^2}\right) = b^2_{6(1+3)}$.
Continuing this procedure, after the k-th refinement step the leftmost vertex is $\beta\left(-\frac{6(1+3+\ldots+3^{k-1})}{3^k}\right) = b^k_{-6(1+3+\ldots+3^{k-1})}$, and the rightmost is $\beta\left(\frac{6(1+3+\ldots+3^{k-1})}{3^k}\right) = b^k_{6(1+3+\ldots+3^{k-1})}$. Thus the support size of β is

$$\begin{aligned}\lim_{k\to\infty}\left[\frac{6(1+3+\ldots+3^{k-1})}{3^k} - \frac{-6(1+3+\ldots+3^{k-1})}{3^k}\right] &= \lim_{k\to\infty}\left[12\left(\frac{1}{3}+\frac{1}{3^2}+\ldots+\frac{1}{3^{k-1}}\right)\right] \\ &= 12\left(\frac{\frac{1}{3}}{1-\frac{1}{3}}\right) = 6.\end{aligned}$$

Since β of the T_4-*scheme* is symmetric, so it is clear that support region is $[-3, 3]$. □

Figure 2 presents comparison among the graphs of basic limit functions generated by the T_4-*scheme* for different values of parameters. The red solid curve is produced for $\alpha = 0$, $\beta = \frac{4}{27}$, $\lambda = \frac{4}{81}$, $\nu = \frac{9}{81}$. Similarly, the solid green and blue curves are produced for $\alpha = -\frac{1}{85}$, $\beta = -\frac{274}{2295}$, $\lambda = -\frac{328}{6885}$, $\nu = -\frac{656}{6885}$ and $\alpha = -\frac{1}{140}$, $\beta = -\frac{47}{540}$, $\lambda = -\frac{383}{11340}$, $\nu = -\frac{383}{5670}$ respectively.

Experiment 4.6. *In this experiment, we graphically analyze the local control property of the* T_4-scheme. *For this purpose we consider control polygon of a cone. In Figure 3*(a)*, we generate limit by the* T_4-scheme *at parametric values* $\alpha = -\frac{1}{83}$, $\beta = -\frac{272}{2241}$, $\lambda = -\frac{326}{6723}$, $\nu = -\frac{652}{6723}$ *and Figure 3*(b) *shows that if one point is moved from its initial place only a small portion of the curve shows an impact while the other curve remains the same.*

4.7. **Polynomial generation property.** Polynomial generation degree of a refinement scheme indicates the highest degree of polynomials that the scheme can generate. To produce C^m-continuous limit curves, polynomial generation of m-th order is an essential condition. A polynomial of degree d can be produced by the non-singular refinement scheme if and only if

$$L(z) = \left(\frac{1+z+z^2}{3}\right)^{d+1} \kappa(z), \quad z \in \mathbb{C}\backslash 0. \tag{4. 12}$$

Here, $\gamma(z) = \left(\frac{1+z+z^2}{3}\right)$ is the smoothing factor. $\kappa(z)$ is the Laurent polynomial with $\kappa(1) = 3$ and does not contain the smoothing factor [15]. Table 3 shows the relationship between the variation of parameters, degeneration of symbol and polynomial generation degree.

4.8. **Polynomial reproduction property and approximating order.** The polynomial reproduction property is important as it indicates that a scheme that can reproduced polynomials up to the degree d possesses an approximation order of $d+1$.

Definition 4.9. *([4]) For a ternary refinement scheme , we denote the parametric shift by $\tau = \frac{L'(1)}{3}$, and attach the data p_n^k for $n, k \in \mathbb{Z}$ to the parameter values as*

$$x_n^k = x_0^k + \frac{n}{3^k} \quad with \quad x_0^k = x_0^{k-1} - \frac{\tau}{3^k}. \tag{4. 13}$$

Theorem 4.10. *([4]). A convergent refinement scheme S with any arity $m \geq 2$ reproduces polynomials of degree $d \geq 1$ with respect to the parametrization in (4. 13) if and only if*

$$\sum_{j\in\mathbb{Z}} j^k L_{mj+i} = \left(\frac{\tau - i}{m}\right)^k,\ i = 0, 1, 2, \ldots, m-1,\ for\ k = 1, 2, 3, \ldots, d, \tag{4. 14}$$

where

$$\tau = \frac{L'(1)}{m}.$$

Theorem 4.11. *([8]). A convergent refinement scheme that reproduces polynomial P_n has an approximation order of $n+1$. In the case of a T_4-*scheme *(where $m = 3$), the (4. 14) takes the form as*

$$\begin{cases} \sum_{j\in\mathbb{Z}} j^k L_{3j} = \left(\frac{\tau}{3}\right)^k, \\ \sum_{j\in\mathbb{Z}} j^k L_{3j+1} = \left(\frac{\tau-1}{3}\right)^k, \\ \sum_{j\in\mathbb{Z}} j^k L_{3j+2} = \left(\frac{\tau-2}{3}\right)^k, \end{cases} \tag{4. 15}$$

for $k = 1, \ldots, d$, and $\tau = \frac{l'(1)}{3}$.

Theorem 4.12. *The T_4-*scheme *has linear polynomial reproduction.*

Proof. The Laurent polynomial of the *T_4-scheme* is

$$\begin{aligned} L(z) \quad = \quad & \left(\frac{1}{243} - \alpha\right)(z^6 + z^{-6}) + \left(\frac{2}{81} - \lambda\right)(z^5 + z^{-5}) + \left(\frac{7}{81} - \nu\right)(z^4 + z^{-4}) \\ & + \left(\frac{50}{243} + 2\alpha - \beta\right)(z^3 + z^{-3}) + \left(\frac{10}{27} - \nu + 2\lambda\right)(z^2 + z^{-2}) + \left(\frac{14}{27} + 2\nu - \lambda\right) \\ & (z + z^{-1}) + \left(\frac{47}{81} - 2\alpha + 2\beta\right). \end{aligned} \tag{4. 16}$$

After differentiating (4. 16) and then evaluating at $z = 1$, leads us to $L^{'}(1) = 0$ and $\tau = 0$. By simplifying the (4. 15) for $\tau = 0$, we obtain the system as given below

$$\begin{cases} (-2)^k l_{-6} + (-1)^k l_{-3} + (1)^k l_3 + (2)^k l_6 = 0, \\ (-2)^k l_{-5} + (-1)^k l_{-2} + (1)^k l_4 = \left(-\frac{1}{3}\right)^k, \\ (-2)^k l_{-4} + (-1)^k l_{-1} + (1)^k l_5 = \left(-\frac{2}{3}\right)^k. \end{cases} \tag{4. 17}$$

□

Corollary 4.13. *The T_4-*scheme *has approximation order 2.*

4.14. **Graphical depiction of polynomial reproduction.** We graphically evaluate the polynomial reproduction of the T_4-*scheme* with different parametric values. The T_4-*scheme* generates a linear polynomial. So it generates limit curves for linear polynomials as given below:

Experiment 4.15. In this experiment, we investigate the polynomial reproduction property of the T_4-*scheme*. Thus, we consider a linear polynomial $y(x) = 2x + 3$. Figure 4 (a)-(c) show that linear behavior for different choices of parameters by setting $\alpha = -\frac{1}{95}$, $\beta = -\frac{284}{2565}$, $\lambda = -\frac{338}{7695}$, $\nu = -\frac{676}{7695}$ (Blue) , $\alpha = -\frac{1}{90}$, $\beta = -\frac{31}{270}$, $\lambda = -\frac{37}{810}$, $\nu = -\frac{37}{405}$ (Red) and $\alpha = -\frac{1}{105}$, $\beta = -\frac{14}{135}$, $\lambda = -\frac{116}{2835}$, $\nu = -\frac{232}{2835}$ (Green) respectively.

5. Fractal property

In this section, we examine the fractal property of the scheme for specific values of the parameters $(\alpha, \beta, \nu) = \left(\frac{1}{243}, \frac{52}{243}, \frac{7}{81}\right)$ which reduces the scheme to a dependence on parameter λ. Assume that b_i^k and b_j^k be arbitrary fixed point two control points, where $k \in \mathbb{Z}$, $k \geq 0$. After the k refinement steps, we must examine how the parameter ν affects the total length of all the tiny edges between two sites throughout an additional k refinement step. To keep things simple, we require to examine the relationship between the two initial points, we must say b_0^0 and b_1^0. For $(\alpha, \beta, \nu) = \left(\frac{1}{243}, \frac{52}{243}, \frac{7}{81}\right)$, the T_4-*scheme* can written as follows

$$\begin{cases} b_{3i}^{k+1} = b_i^k, \quad 0 \leq i \leq 3^k n, \\ b_{3i+1}^{k+1} = u_0 b_{i-1}^k + u_1 b_i^k + u_2 b_{i+1}^k + u_3 b_{i+2}^k, \quad 0 \leq i \leq 3^k n, \\ b_{3i+2}^{k+1} = u_3 b_{i-1}^k + u_2 b_i^k + u_1 b_{i+1}^k + u_0 b_{i+2}^k, \quad 0 \leq i \leq 3^k n, \end{cases} \tag{5. 18}$$

where

$$u_0 = 0, u_1 = \frac{56}{81} - \lambda, u_2 = \frac{23}{81} + 2\lambda, u_3 = \frac{2}{81} - \lambda.$$

We know that based on the interpolatory refinement rule (5. 18)

$$b_0^k \equiv b_0^0,$$

also from (5. 18), we get

$$\begin{cases} b_1^{k+1} = u_0 b_{-1}^k + u_1 b_0^k + u_2 b_1^k + u_3 b_2^k, \\ b_{-1}^{k+1} = u_3 b_{-2}^k + u_2 b_{-1}^k + u_1 b_0^k + u_0 b_1^k. \end{cases} \tag{5. 19}$$

We refer three typical edge vectors

$$V_k = b_1^k - b_0^k, \quad S_k = b_2^k - b_1^k, \quad R_k = b_3^k - b_2^k.$$

The difference equation of edge vectors can be obtained with the help of following vectors

$$U_k = b_1^k - b_{-1}^k, \quad W_k = b_0^k - b_{-1}^k, \quad Z_k = b_2^k - b_{-2}^k.$$

Consider vector U_k, such as

$$U_{k+1} = b_{+1}^{k+1} - b_{-1}^{k+1}, \tag{5. 20}$$

after simplifying , we get

$$U_{k+1} - (u_2 - u_0) U_k = u_3 Z_k. \tag{5. 21}$$

Similarly, we obtain

$$Z_{k+1} - u_0 Z_k = (u_1 - u_3)\, U_k \ . \tag{5. 22}$$

By using (5. 21) and (5. 22), we obtain the solution of U_k

$$U_k = c_1 r_1^k + c_2 r_2^k, \tag{5. 23}$$

where

$$r_1 = \frac{1}{3}, \quad r_2 = -\frac{4}{81} + 2\lambda,$$

$$c_1 = -\frac{(2-81\lambda)(b_2^0 - b_{-2}^0) + 27(b_1^0 - b_{-1}^0)}{-31 + 162\lambda},$$

$$and \quad c_2 = -\frac{(2-81\lambda)\left((b_2^0 - b_{-2}^0) - 2(b_1^0 - b_{-1}^0)\right)}{-31 + 162\lambda}.$$

Similarly, we obtain the solution of Z_k

$$Z_k = d_1 A_1^k + d_2 r_1^k + d_3 r_2^k, \tag{5. 24}$$

where

$$A_1 = 0, \quad d_1 = 0, \quad d_2 = 2c_1, \quad and \quad d_3 = -\frac{27}{2-81\lambda} c_2.$$

Consider edge vector V_k, such as

$$V_{k+1} = b_1^{k+1} - b_0^{k+1},$$

after simplification, we get

$$V_{k+1} - (u_1 - 1)\, V_k = -u_0 U_k + u_3 S_k \ . \tag{5. 25}$$

Similarly, we obtain

$$S_{k+1} - (u_0 - u_3)\, S_k = (u_1 - u_2)\, V_k - (u_0 - u_3)\, U_k. \tag{5. 26}$$

By using (5. 21) and (5. 25) in (5. 26), we get

$$\begin{aligned} &V_{k+2} - \left(\frac{23}{81} + 2\lambda\right) V_{k+1} - \left(2\lambda^2 - \frac{62\lambda}{81} + \frac{116}{6561}\right) V_k \\ &= -\left(\lambda^2 - \frac{4\lambda}{81} + \frac{4}{6561}\right)(c_1 r_1^k + c_2 r_2^k), \end{aligned} \tag{5. 27}$$

after simplifying above expression, we obtain the solution of V_k

$$V_k = a_1 r_3^k + a_2 r_4^k + a_3 r_1^k + a_4 r_2^k, \tag{5. 28}$$

where

$$r_3 = \frac{1}{162}\left((23 + 162\lambda) + \sqrt{993 - 12636\lambda + 78732\lambda^2}\right),$$

$$r_4 = \frac{1}{162}\left((23 + 162\lambda) - \sqrt{993 - 12636\lambda + 78732\lambda^2}\right),$$

$$a_3 = \frac{1}{2} c_1, \quad a_4 = \frac{1}{2} c_2,$$

$$\begin{aligned} a_1 \quad = \quad & \frac{1}{4\sqrt{993 - 12636\lambda + 78732\lambda^2}} \left((4 - 162\lambda)\left(b_2^0 + b_{-2}^0\right) + (23 + 162\lambda + \right. \\ & \left. \sqrt{993 - 12636\lambda + 78732\lambda^2}\right)\left(b_1^0 + b_{-1}^0\right) - \left(54 + 2\sqrt{993 - 12636\lambda + 78732\lambda^2}\right) b_0^0\Big), \end{aligned}$$

and

$$a_2 = \frac{1}{4\sqrt{993-12636\lambda+78732\lambda^2}}\left((-4+162\lambda)\left(b_2^0+b_{-2}^0\right)+(-23-162\lambda+\sqrt{993-12636\lambda+78732\lambda^2}\right)\left(b_1^0+b_{-1}^0\right)+\left(54-2\sqrt{993-12636\lambda+78732\lambda^2}\right)b_0^0\Big).$$

Similarly, we obtain the solution of S_k

$$S_k = m_0\left(-\frac{2}{81}+\lambda\right)^k + m_1 r_1^k + m_2 r_2^k + m_3 r_3^k + m_4 r_4^k, \tag{5. 29}$$

where

$$m_0 = 0, \quad m_1 = a_3, \quad m_2 = \frac{(29-81\lambda)}{(-2+81\lambda)}a_4, \quad m_3 = \frac{6\,(11-81\lambda)}{27+\sqrt{993-12636\lambda+78732\lambda^2}}a_1,$$
$$\text{and} \quad m_4 = \frac{-6\,(11-81\lambda)}{-27+\sqrt{993-12636\lambda+78732\lambda^2}}a_2.$$

Consider vector R_k, such as

$$R_{k+1} = b_3^{k+1} - b_2^{k+1},$$

after simplifying, we get

$$R_{k+1} = u_3 U_k + u_2 V_k - u_0 S_k,$$

By using (5. 19), (5. 28) and (5. 29), we obtain the solution of R_k

$$R_k = I_0\left(-\tfrac{2}{81}+\lambda\right)^k + I_1 r_1^k + I_2 r_2^k + I_3 r_3^k + I_4 r_4^k, \tag{5. 30}$$

where

$$I_0 = 0, \quad I_1 = a_3, \quad I_2 = \frac{-27}{(4-162\lambda)}a_4, \quad I_3 = \left(\frac{23+162\lambda}{81 r_3}\right)a_1,$$
$$and \quad I_4 = \left(\frac{23+162\lambda}{81 r_4}\right)a_2.$$

Theorem 5.1. *For $\lambda \in \left(-\frac{23}{162}, \frac{2}{81}\right)$, limit curves of the refinement scheme (5. 18) is fractal.*

Proof. When $\lambda \in \left(-\frac{23}{162}, \frac{2}{81}\right)$ it may be concluded that after k refinement steps there are 3^k small edge vectors between the initial control points b_0^0 and b_1^0 can be written as

$$E_i^k = b_i^k - b_{i-1}^k = a_{1i}\,(A_2)^k + a_{2i} r_1^k + a_{3i} r_2^k + a_{4i} r_3^k + a_{5i} r_4^k \quad i = 1, 2, 3 \cdots 3^k,$$

where $a_{j,i} \neq 0,$ for $j = 1, 2, 3, 4, 5$. In this case, we see that $|r_3| > |A_2|, |r_3| > |r_1|, |r_3| > |r_2|, |r_3| > |r_4|$.
Let $|E_i^k| = min_{1,2,3\cdots 3^k}|E_i^k|$, then we have

$$\begin{aligned}\sum_{i=1}^{3^k}|E_i^k| \geq 3^k|E_{i0}^k| &= 3^k|a_{1i}\,(A_2)^k + a_{2i} r_1^k + a_{3i} r_2^k + a_{4i} r_3^k + a_{5i} r_4^k| \\ &= 3^k\,|r_1|^k\left|a_{1i}\left\{\frac{A_2}{r_3}\right\}^k + a_{2i}\left\{\frac{r_1}{r_3}\right\}^k + a_{3i}\left\{\frac{r_2}{r_3}\right\}^k + a_{4i} + a_{5i}\left\{\frac{r_4}{r_3}\right\}^k\right| \\ &\to \infty\,(k\to\infty).\end{aligned}$$

So for $\lambda \in \left(-\frac{23}{162}, \frac{2}{81}\right)$, limit curves of the scheme are fractal curves. □

5.2. **Graphical depiction of fractal generation.** In this section, variety of fractal curves is produced by the T_4-*scheme*. The performance of the scheme is evaluated for various values of parameter λ within the the fractal range. Additionally, when one or more parameters are provided, the fractal characteristic can be further investigated. The results display the excellent performance for generating stunning fractals by the T_4-*scheme*.

Experiment 5.3. In this experiment, we show the fractal behavior of the T_4-*scheme* at different iteration levels. Figures $5(a)$-$5(c)$ represent intricate fractal curves corresponding to $\lambda = -0.0811$ at 2^{nd}, 3^{rd} and 4^{th} refinement levels respectively. These representations show that after increasing refinement levels more aesthetic fractals are produced.

Experiment 5.4. In this experiment, we use different values of parameter to display the fractal behavior of the proposed scheme on a control polygon. Fractal curves shown in Figures $6(a)$ and $6(c)$ are obtained for $\lambda = -0.095$ and $\lambda = -0.0825$ respectively. Whereas the box part of these figures have been zoomed in Figures $6(b)$ and $6(d)$ respectively. These images indicate that the smaller details of the fractal look like the larger structure repeated recursively at different scales which shows the self-similar property of the fractal curve.

Experiment 5.5. In this experiment, we use different values of parameter to display the fractal behavior of the T_4-*scheme* on the same control polygon. Figure $7(a)$-$7(c)$ display the fractal behavior for the different values of parameters. The given scheme can efficiently and accurately produce fractal curves by setting adequate parameters. Figure 7 shows fractal curves with different values of parameters.

6. Numerical experiments and conclusions

A control polygon is a series of points that provides a simple and intuitive way to manipulate the shape by adjusting the positions of its points. In this section, we illustrate the graphical behavior of the scheme T_4-*scheme* on several polygons. The beauty of the T_4-*scheme* is that it is a combined scheme, which offers the greatest flexibility in generating smooth interpolating and approximating limit curves respectively. Therefore, we demonstrate that for appropriate choices of parameters the resulting limit curves display interproximal behavior.

Experiment 6.1. In this experiment, we illustrates the behavior of the T_4-*scheme* on a closed control polygon at different refinement levels. Figures$8(a) - (c)$ illustrate the behavior of scheme at 1st, 2nd and 3rd refinement levels for $\alpha = -\frac{1}{92}, \beta = -\frac{281}{2484}, \lambda = -\frac{335}{7452}, \nu = -\frac{335}{3726}$.

Experiment 6.2. In this experiment, we use different values of parameters to display the approximating and interpolating behavior of the T_4-*scheme* on a closed control polygon. Green limiting curve illustrates the behavior of scheme when $\alpha = -\frac{1}{86}, \beta = -\frac{275}{2322}, \lambda = -\frac{329}{6966}, \nu = -\frac{329}{3483}$. Purple limiting curve illustrates the behavior of scheme when $\alpha = -\frac{1}{106}, \beta = -\frac{295}{2862}, \lambda = -\frac{349}{8586}, \nu = -\frac{349}{4293}$. Blue limiting curve illustrates the behavior of scheme when $\alpha = -\frac{1}{146}, \beta = -\frac{335}{3942}, \lambda = -\frac{389}{11862}, \nu = -\frac{389}{5913}$. Red limiting curve illustrates the behavior of interpolating scheme when $\alpha = 0, \beta = \frac{4}{27}, \lambda = \frac{2}{81}, \nu = \frac{1}{27}$.

Figure $9(a)$ presents the comparison of these limit curves and Figure $9(b)$ presents the magnified view of this comparison.

Experiment 6.3. In this experiment, we present comparative analysis of the T_4-*scheme* with some existing refinement schemes. Figure $10(a)$ illustrates the behavior of scheme [3] when $\omega = \frac{1}{64}$. Figures $10(b)$ illustrates the behavior of scheme [26] when $\mu = \frac{2}{32}$. Figure $10(c)$ illustrates the behavior of the T_4-*scheme* when $\alpha = \frac{1}{81}, \beta = \frac{4}{81}, \lambda = \frac{2}{81}, \nu = \frac{4}{81}$. It is easy to observe that the T_4-*scheme* has better control over the control polygon as compared to other existing schemes.

7. Conclusion

In this paper, we have introduced a novel combined 4-point ternary refinement scheme with four parameters. The scheme attains C^4 convergence while maintaining a compact support $[-3, 3]$. The inclusion of parameters enhances the flexibility of scheme, allowing various parameter adjustments to achieve specific levels of continuity. Detailed analysis are provided to examine key properties of the scheme. Additionally, the fractal behavior of the refinement scheme is investigated, with particular parameter selections enabling the effective construction of fractal curves. Moreover, the application of fractal curves produced by the proposed scheme demonstrates its capacity to generate dense fractal depths, opens new possibilities for artistic expression and scientific visualization. Additionally, numerical examples of the proposed scheme illustrate the fact that the parameters selection significantly impacts the curve shape. Alternative parameters tend to produce inwardly shrinking curves, while positive parameters lead to outward expansion. This flexibility allows designers to fine-tune the appearance of their models according to their requirements by choosing appropriate parameters. These comprehensive analysis collectively contribute to the better understanding of the proposed scheme.

CRediT AUTHORSHIP CONTRIBUTION STATEMENT

Pakeeza Ashraf: Conceptualization, Methodology, Validation, Investigation, Data curation, Project Administration, Writing-original draft, Supervision. Fatima Rasheed: Methodology, Validation, Investigation, Data curation, Writing-original draft, Software.

CONFLICT OF INTERESTS

The authors declare that there is no conflict of interest regarding the publication of this article and regarding the funding that they have received.

FUNDING

This research is not funded by any government or private organization.

REFERENCES

[1] P. Ashraf, Nawaz, B., Baleanu, D., Sooppy Nisar, K., Ghaffar, A., Khan, M. A. A., and Akram, S., *Analysis of geometric properties of ternary four-point rational interpolating subdivision scheme*, Mathematics, **8**, No. 3 (2020) 338.

[2] M. Asghar and Mustafa, G., *Stationary and non-stationary univariate subdivision schemes*, Punjab Univ. J. Math., **50**, No. 3 (2018) 25–42.

[3] H. Cao and Tan, J., *A binary five-point relaxation subdivision scheme*, J. Inf. Comput. Sci., **10**, No. 18 (2013) 5903–5910.

[4] C. Conti and Hormann, K., *Polynomial reproduction for univariate subdivision schemes of any arity*, J. Approx. Theory, **163**, No. 4 (2011) 413–437.

[5] G. Deslauriers and Dubuc, S., *Symmetric iterative interpolation processes*, Constructive Approx., **5**, No. 1 (1989) 4968.

[6] N. Dyn, Levin, D., and Gregory, J. A., *A 4-point interpolatory subdivision scheme for curve design*, Comput. Aided Geom. Design, **4**, No. 4 (1987) 257–268.

[7] N. Dyn, *Subdivision schemes in CAGD*, Adv. Numer. Anal., **2**, (1992) 36–104.

[8] N. Dyn, *Interpolatory subdivision schemes*, Tutorials on Multiresolution in Geometric Modelling, **1**, (2002) 25–50.

[9] L. Gori, Pitolli, F., and Santi, E., *On a class of shape-preserving refinable functions with dilation 3*, J. Comput. Appl. Math., **245**, No. 1 (2013) 62–74.

[10] M. Hassan, and Dodgson, N. A., *Ternary and three-point univariate subdivision schemes*, Univ. of Cambridge, Comput. Lab., Tech. Rep. UCAM-CL-TR-520, **1**, (2001).

[11] F. Khan, Omar, M., and Mustafa, G., *Generalized family of approximating schemes based on Newton interpolating polynomials and its error analysis*, Punjab Univ. J. Math., **51**, No. 6 (2020)

[12] K.P. Ko, Lee, B. G., and Yoon, G. J., *A ternary 4-point approximating subdivision scheme*, Appl. Math. Comput., **190**, No. 2 (2007) 1563–1573.

[13] A. Levin, *Combined refinement schemes for the design of surfaces satisfying boundary conditions*, Comput. Aided Geom. Design, **16**, No. 5 (1999) 345–354.

[14] J.A. Lian, *On a-ary subdivision for curve design III. $2m$-point and $(2m+1)$-point interpolatory schemes*, Appl. Appl. Math., **4**, No. 2 (2009) 434-444.

[15] Z. Luo and Qi, W., *On interpolatory subdivision from approximating subdivision scheme*, Appl. Math. Comput., **220**, No. 1 (2013) 339–349.

[16] G. Mustafa, Ghaffar, A., and Khan, F., *The odd-point ternary approximating schemes*, Am. J. Comput. Math., **1**, No. 2 (2011) 111.

[17] P. Novara, and Romani, L., *Complete characterization of the regions of C^2 and C^3 convergence of combined ternary 4-point subdivision schemes*, Appl. Math. Lett., **62**, No. 1 (2016) 84–91.

[18] J. Pan, Lin, S., and Luo, X., *A combined approximating and interpolating subdivision scheme with C^2 continuity*, Appl. Math. Lett., **25**, No. 12 (2012) 2140–2146.

[19] K. Peng, Tan, J., Li, Z., and Zhang, L., *Fractal behavior of a ternary 4-point rational interpolation subdivision scheme*, Math. Comput. Appl., **23**, No. 4 (2018) 65.

[20] K. Rehan and Sabri, M. A., *A combined ternary 4-point subdivision scheme*, Appl. Math. Comput., **276**, No. 1 (2016) 278–283.

[21] K. Rehan and Siddiqi, S. S., *A combined binary 6-point subdivision scheme*, Appl. Math. Comput., **270**, No. 1 (2015) 130–135.

[22] S.S. Siddiqi and Rehan, K., *Ternary $2N$-point Lagrange subdivision schemes*, Appl. Math. Comput., **249**, No. 1 (2014) 444–452.

[23] W.S.Yao, Ashraf, P., Ghaffar, A., Kousar, M., Inc, M., and Nigar, N., *Fractal and convexity analysis of the quaternary four-point scheme and its applications*, Fractals, **31**, No. 10 (2023) 2340088.

[24] L. Zhang, Ma, H., Tang, S., and Tan, J., *A combined approximating and interpolating ternary 4-point subdivision scheme*, J. Comput. Appl. Math., **349**, No. 1 (2019) 563–578.

[25] Z. Zhang, and Zheng, H. , *A class of non-stationary ternary 4-point subdivision schemes based on iterations*, Punjab Univ. J. Math. **57**, No. 3 (2025) 340–352.

[26] H. Zheng, Ye, Z., Lei, Y., and Liu, X., *Fractal properties of interpolatory subdivision schemes and their application in fractal generation*, Chaos Solitons Fractals, **32**, No. 1 (2007) 113–123.

TABLE 1. *Special cases of the T_4-*scheme*. Here I stands for interpolating scheme and A stands for approximating scheme.*

Scheme	Continuity	Type	Support	Parameters
2-pt [9]	C^2	A	$[-\frac{3}{2},\frac{3}{2}]$	$(\alpha,\beta,\nu,\lambda)=(\frac{1}{243},\frac{52}{243}-\frac{1}{9}\alpha,$ $,\frac{7}{81},\frac{2}{81})$
3-pt [16]	C^2	A	$[-2,2]$	$(\alpha,\beta,\nu,\lambda)=(\frac{1}{243},\frac{1}{9}(\frac{25}{27}-\frac{1}{4}\alpha),$ $\frac{1}{9}(\frac{7}{9}-\frac{1}{4}\alpha),\frac{2}{81})$
4-pt [22]	C^3	A	$[-3,3]$	$(\alpha,\beta,\nu,\lambda)=(\frac{1}{243}+\mu,\frac{52}{243}-2\mu,\frac{4}{27},\frac{2}{27})$
combined 4-pt [18]	C^1 C^3	I A	$[-3,3]$	$(\alpha,\beta,\nu,\lambda)=(\frac{1}{243},\frac{16}{243}-\frac{1}{27}\alpha,\frac{4}{27}-\beta(1-\alpha)$ $,\frac{2}{27}-\beta(1-\alpha))$
combined 4-pt [17]	C^2 C^3	I A	$[-\frac{5}{2},\frac{5}{2}]$	$(\alpha,\beta,\nu,\lambda)=(\frac{1}{243},\frac{25}{243}+\alpha,\frac{7}{81}-\beta$ $,\frac{2}{81}-\gamma)$

TABLE 2. *The relationship between continuity order and variation of parameters.*

Continuity	Variation of parameters
C^0	$\{\alpha,\beta,\nu,\lambda\in\mathbb{R},\max\{\lvert\frac{1}{243}-\alpha\rvert+\lvert\frac{10}{81}-\beta+\alpha+\nu\rvert+\lvert\frac{5}{27}-\nu+\lambda+\beta-\alpha\rvert$ $+\lvert\frac{5}{243}-\lambda-\alpha\rvert,\lvert\frac{17}{81}-2\lambda+2\nu\rvert+2\lvert\frac{5}{81}-\nu+\lambda\rvert\}<1\}$
C^1	$\{\alpha,\beta,\nu,\lambda\in\mathbb{R},\nu=0,\max\{\lvert\frac{1}{81}-3\alpha\rvert+\lvert\frac{16}{81}-3\beta-3\lambda\rvert+\lvert\frac{10}{81}+6\lambda-3\alpha\rvert,$ $\lvert\frac{19}{81}+6\beta\rvert+2\lvert\frac{4}{81}-3\lambda+6\alpha\rvert\}<1\}$
C^2	$\{\alpha,\beta,\nu,\lambda\in\mathbb{R},\beta=\lambda+\nu-2\alpha,\max\{2\lvert\frac{1}{27}-9\alpha\rvert+\lvert\frac{7}{27}+18\alpha+18\nu-36\lambda\rvert,$ $\lvert\frac{1}{9}-9\lambda+27\alpha\rvert+\lvert\frac{2}{9}-9\nu+27\lambda-27\alpha\rvert\}<1\}$
C^3	$\{\alpha,\beta,\nu,\lambda\in\mathbb{R},\beta=3\lambda-2\alpha,\nu=2\lambda,\max\{\lvert\frac{1}{9}-27\alpha\rvert+\lvert\frac{2}{9}+108\alpha-27\lambda\rvert,$ $\lvert\frac{1}{3}-162\alpha+54\lambda\rvert\}<1\}$
C^4	$\{\alpha,\beta,\nu,\lambda\in\mathbb{R},\beta=7\alpha,\lambda=3\alpha,\nu=6\alpha,-\frac{1}{81}<\alpha<0\}$

TABLE 3. *The relationship between variation of parameters, degeneration of symbol and polynomial generation degree (G(d)).*

Variation of parameters	Degeneration of symbol	G(d)
$\{\alpha,\beta,\nu,\lambda\in\mathbb{R},\nu=0\}$	$L(z)=\gamma(z)^2\kappa_2(z)$	1
$\{\alpha,\beta,\nu,\lambda\in\mathbb{R},\beta=\lambda+\nu-2\alpha\}$	$L(z)=\gamma(z)^3\kappa_3(z)$	2
$\{\alpha,\beta,\nu,\lambda\in\mathbb{R},\beta=3\lambda-2\alpha,\nu=2\lambda\}$	$L(z)=\gamma(z)^4\kappa_4(z)$	3
$\{\alpha,\beta,\nu,\lambda\in\mathbb{R},\beta=7\alpha,\lambda=3\alpha,\nu=6\alpha\}$	$L(z)=\gamma(z)^5\kappa_5(z)$	4

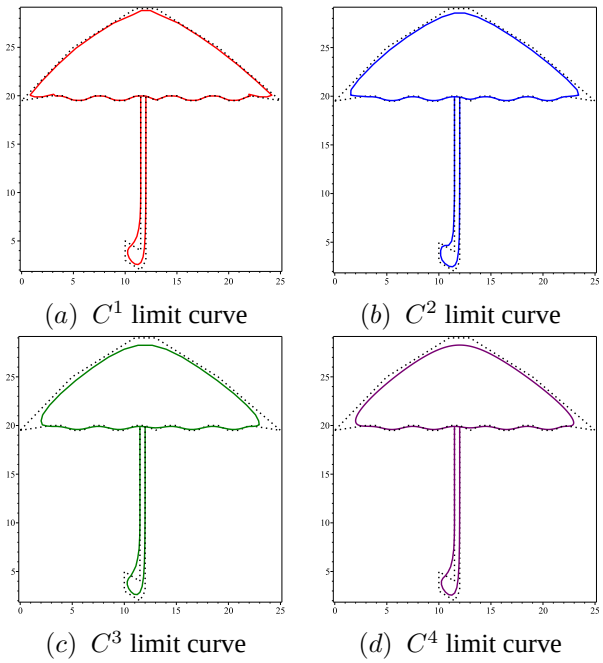

(a) C^1 limit curve (b) C^2 limit curve

(c) C^3 limit curve (d) C^4 limit curve

FIGURE 1. *Umbrella curves with different continuity orders .*

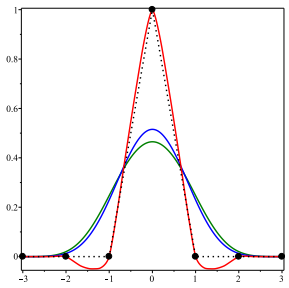

FIGURE 2. *Results of the* T_4-scheme *for basic limit functions with different parametric values after fourth refinement level .*

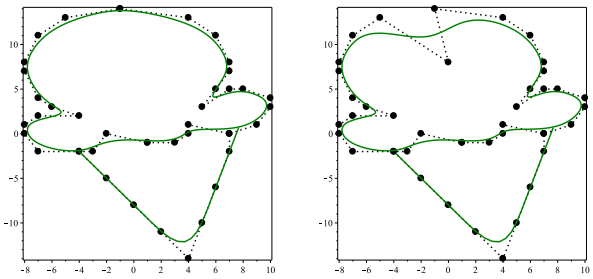

(a) (b)

FIGURE 3. *The solid line represents the result fitted by the* T_4-scheme *after the fourth refinement level.*

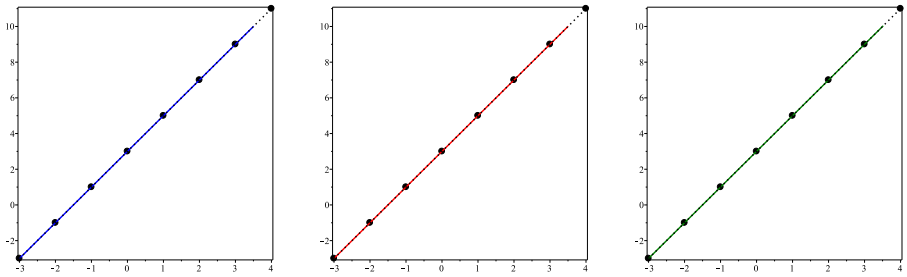

(a) (b) (c)

FIGURE 4. *The dotted and the solid lines represents the initial control polygon and control points respectively. The solid lines with different colors characterize curves fitted by the* T_4-scheme *with different parametric values after the third refinement level.*

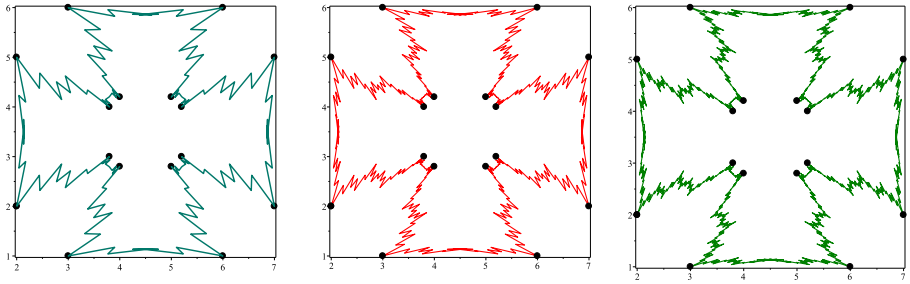

(a) (b) (c)

FIGURE 5. *The behavior of limit curves generated by fractal curve for the different refinement levels.*

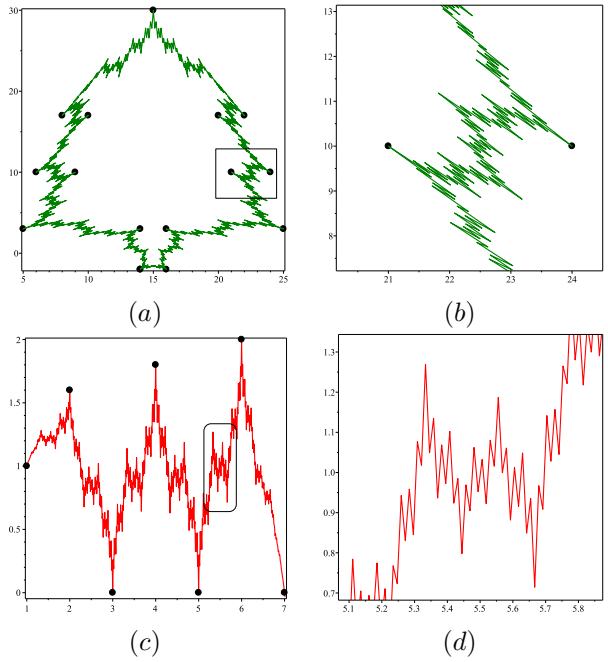

FIGURE 6. *The behaviour of limit curves generated by fractal curve for the different values of* λ

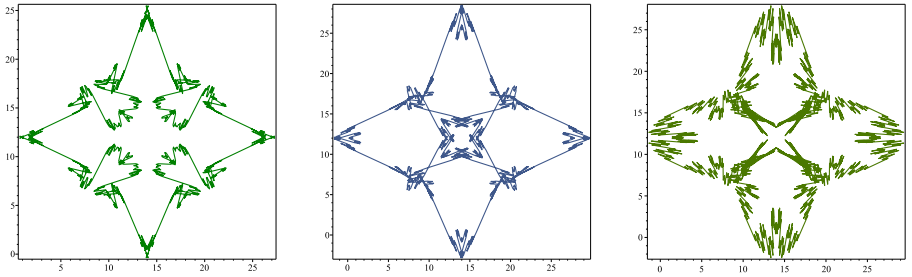

(a) $\alpha = 0, \beta = \frac{13}{81}$, $\lambda = -\frac{17}{81}, \nu = \frac{8}{81}$

(b) $\alpha = 0, \beta = \frac{5}{27}$, $\lambda = -\frac{5}{81}, \nu = \frac{7}{27}$

(c) $\alpha = \frac{1}{81}, \beta = -\frac{1}{27}$, $\lambda = \frac{1}{162}, \nu = \frac{7}{27}$

FIGURE 7. *The behaviour of limit curves generated by fractal curve for the different values of parameters.*

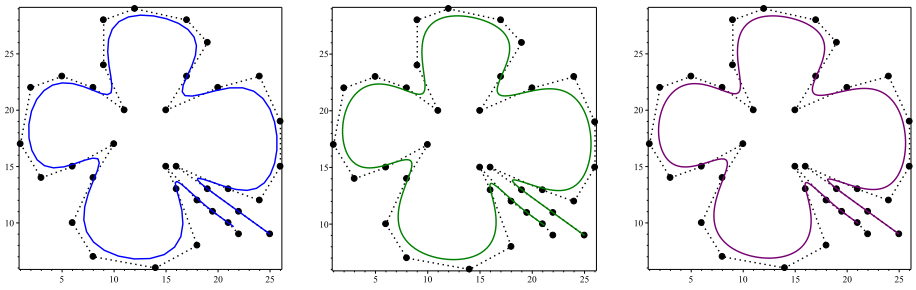

(a) (b) (c)

FIGURE 8. *The behaviour of limit curves generated at different refinement levels.*

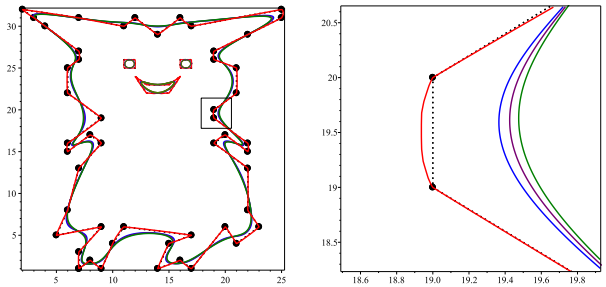

(a) (b)

FIGURE 9. *The behavior of limiting curves generated by the* T_4-scheme *for the different values of parameters, (a) illustrates the comparison of the limit curves and (b) presents the zooming area.*

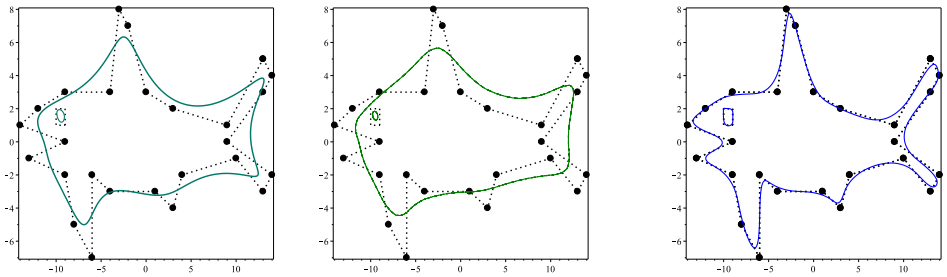

(a) limit curve of [3] (b) limit curve of [26] (c) Limit curve of the T_4-*scheme*

FIGURE 10. *Comparison of limit curves generated by the* T_4-scheme *with other existing refinement schemes*